

Are Vortex Quasi-Crystals New Phases of Vortex Matter?

Wei Zhang and C. A. R. Sá de Melo

School of Physics, Georgia Institute of Technology, Atlanta, Georgia 30332

(Dated: November 1, 2018)

There seems to be a one to one correspondence between the phases of atomic and molecular matter (AMOM) and vortex matter (VM) in superfluids and superconductors. Crystals, liquids and glasses have been experimentally observed in both AMOM and VM. However, quasi-crystals also exist in AMOM, thus a new phase of vortex matter is proposed here: the vortex quasi-crystal. It is argued that vortex quasi-crystals are stabilized due to imposed quasi-periodic potentials in large samples or due to boundary and surface energy effects for samples of special shapes and sizes. For finite size samples, it is proposed that a phase transition between a vortex crystal and a vortex quasi-crystal occurs as a function of magnetic field and temperature as the sample size is reduced.

PACS numbers: 74.25.Op, 74.25.-q, 74.25.Dw

The general subject of vortex physics in superconductors is quite interesting since there seems to be a large variety of possible equilibrium vortex phases in superconductors [1]. The term “vortex matter” has been coined to emphasize the complexity and diversity of vortex phases in superconductors when compared to atomic and molecular matter. One can think of a one to one correspondence between phases in atomic and molecular matter (AMOM) and phases in vortex matter (VM). A liquid in AMOM corresponds to a vortex liquid in VM; a crystalline lattice in AMOM corresponds to a vortex lattice in VM; an amorphous or glassy solid in AMOM corresponds to an amorphous or glassy vortex system in VM. However, among all the possibilities discussed in the vortex matter literature, a very interesting one is missing: the vortex quasi-crystal. Quasi-crystals in AMOM were experimentally discovered several years ago [2], but there are no corresponding experiments for vortex matter. Thus, the present paper is dedicated to the proposal of vortex quasi-crystalline phases. It will be argued that vortex quasi-crystals maybe stabilized either by imposing quasi-periodic potentials or by boundary effects and surface energies in finite systems.

The central question of this manuscript is: are vortex quasi-crystals new phases of vortex matter? If so, what suggestions can be given to experimentalists to help in the search for such phases? It must be emphasized that these questions will be addressed here on a preliminary basis, and further detailed work will be necessary. In order to consider the possibility of a vortex quasi-crystal one must seek under what conditions a quasi-crystalline arrangement is at all possible. A definite possibility is to argue that a stable vortex quasi-crystal can arise for an imposed quasi-periodic potential in a multilayered structure, like for instance in the case of a superconductor that is grown on top of a flat quasi-crystal surface. Another possibility is to create a quasi-periodic optical lattice with laser beams, trap and cool atoms, and produce vortex quasi-crystals in Bose or Fermi superfluids. This experiment is natural since the production of vortex lat-

tices in superfluid Bose or Fermi ultra-cold atoms has become standard [3, 4]. However, in this manuscript, we concentrate on the possibility of stabilizing vortex quasi-crystals only due to boundary effects in finite superconducting samples, where the sample size and shape play an important role. This option is motivated by recent experimental studies of the vortex structure in disk, triangular, square, and star-shaped mesoscopic samples [5, 6, 7, 8]. Present technology should allow the preparation of pentagonal (pentagon-cylinders) or decagonal (decagonal-cylinders) samples as potential candidates to produce 5-fold vortex quasi-crystals. If boundaries are important then in the thermodynamic limit of infinite volume it is generally difficult to produce vortex quasi-crystalline order, unless a quasi-periodic potential is imposed, as mentioned above.

This possibility is considered here under the following program. In this manuscript only the case of an isotropic type II superconductor in a magnetic field is considered. First, the bulk free energy is calculated for a triangular, a square and a 5-fold quasi-crystal array. The 5-fold quasi-crystal array is modeled by a Penrose tiling of the plane. It is shown that the Penrose tile array (vortex quasi-crystal) has a bulk free energy which is just a few percent higher than the triangular array. Second, instead of considering an infinite (bulk) system, a pentagon cylinder sample is discussed. The pentagon cylinder has a pentagonal cross-section (in the xy plane) with side dimension ℓ , and with height L along the z direction. In this case, when the sample size gets smaller the contribution of the boundaries (surface energy) to the total free energy of the system becomes more important. The surface energy is highly sensitive to the symmetry and to the surface area of the boundaries. Taking into account the surface free energies, it is shown that the Penrose tile (vortex quasi-crystal) has lower free energy than the triangular lattice in certain regions of the magnetic field versus temperature phase diagram. This is suggestive that a “first order phase transition” may occur between the triangular lattice and the Penrose tiling

(vortex quasi-crystal) [9].

For simplicity, the starting point of the analysis to follow is the Ginzburg-Landau (GL) free energy density

$$\Delta F_s = F_1 + \frac{1}{2m} \left| \left(-i\hbar\nabla - \frac{2e\mathbf{A}}{c} \right) \Psi(\mathbf{r}) \right|^2 + \frac{H^2}{8\pi} \quad (1)$$

for a bulk isotropic superconductor with no disorder, where $\Delta F_s = F_s - F_n$ is the free energy density difference between the superconducting state (F_s) and the normal state (F_n), and $F_1 = \alpha|\Psi(\mathbf{r})|^2 + \beta|\Psi(\mathbf{r})|^4/2$. It is useful to introduce the dimensionless quantities $f = \Psi\sqrt{-\beta/\alpha}$, $\boldsymbol{\rho} = \mathbf{r}/\lambda(T)$, $\mathcal{A} = 2\pi\xi(T)\mathbf{A}/\Phi_0$, and $\mathcal{H} = 2\pi\xi(T)\lambda(T)H/\Phi_0$, where λ is the penetration depth, ξ is the coherence length, and $\Phi_0 = hc/2e$ is the unit flux. Here, $f = f_0 \exp(i\phi)$, and $\mathcal{A} = \mathcal{A}_0 + \nabla\phi/\kappa$ with $\kappa = \lambda/\xi$ is the GL parameter. Notice that when $f_0 = 1$ the system is fully superconducting, and when $f_0 = 0$ the system is normal, thus $f_0 \leq 1$ always. Considering the minimization of free energy density with respect to \mathcal{A} and Ψ it is easy to arrive at equations for the dimensionless functions \mathcal{H} and f_0 . The microscopic field is

$$\mathcal{H}(x, y) = \kappa \left[1 + \frac{H - H_{c2}}{H_{c2}} \right] - \frac{g(x, y)}{2\kappa}, \quad (2)$$

with \mathbf{H} parallel to the \mathbf{z} direction, and the equation for f_0 can be written as

$$\nabla^2(\log g) + 2\kappa^2 = 0, \quad (3)$$

where $g = f_0^2$ is a positive definite function. Notice that $\mathcal{H} = \kappa$ for $H = H_{c2}$ and $f_0 = 0$ ($g = 0$). The most general solution of Eq. (3) has the form [10]

$$g(x, y) = \exp[-\kappa^2(x^2 + y^2)/2] \exp[\gamma(x, y)], \quad (4)$$

where $\gamma(x, y)$ satisfies Laplace's equation $\nabla^2\gamma(x, y) = 0$. This means that $\gamma(x, y)$ is a harmonic function excluding the locations of vortices, and can be expressed as the real part of an analytic function of $z = x + iy$. This observation has very important consequences for the microscopic field profile $\mathcal{H}(x, y)$ of Eq. (2), which depends strongly on the structure of $g(x, y)$.

The bulk Gibbs free energy density can be expressed as [11]

$$G_s(H, T) = G_n(H, T) - \frac{1}{8\pi} \frac{(H_{c2} - H)^2}{(2\kappa^2 - 1)\beta}, \quad (5)$$

where the parameter $\beta = \langle g^2 \rangle / \langle g \rangle^2$ is a geometrical factor independent of κ . The notation $\langle \dots \rangle$ indicates average over volume. It is important to notice that $\beta \geq 1$ no matter what is the form of $g(x, y)$ because of the Schwartz inequality. In addition, notice that the Gibbs free energy above is a minimum, whenever β reaches its minimum value.

For the purpose of calculating the parameter β and the free energies corresponding to different vortex configurations, the analytical structure of $g(x, y)$ in the complex plane is used to rewrite it as

$$g(z, \bar{z}) = \exp(-\kappa^2 z \bar{z}/2) |P(z)|, \quad (6)$$

where $P(z) = \mathcal{N} \prod_{i=1}^M (z - z_i)$. Here each z_i corresponds to a zero of g in the complex plane, and M is the number of zeros. The zeros z_i indicate the location of vortices. From now on it is assumed that there is only one vortex with flux Φ_0 at each position z_i , i.e., each zero is non-degenerate. In this case, M corresponds to the number of vortices, and thus the total flux threading the sample is $\Phi = M\Phi_0$. The normalization coefficient \mathcal{N} just guarantees that $g(z, \bar{z}) \leq 1$. Depending on the locations of the zeros of $g(z, \bar{z})$, it is possible to study several possibilities of periodic and quasi-periodic vortex arrangements. In this study only vortex crystals corresponding to triangular and square lattices and vortex quasi-crystals corresponding to the 5-fold Penrose tiling of the plane are considered. Both the square lattices and triangular lattices can be generated via the tiling method, i.e., via the periodic arrangements of identical square tiles or identical lozenges of internal angles (60° and 120°). The Penrose lattice, however, requires quasi-periodic arrangements of two types of tiles (lozenges), one with internal angles 36° and 144° and the other with internal angles 72° and 108°. Using the representation in Eq. (6), the values of β for the triangular, square and Penrose tiling are respectively $\beta_3 = 1.16$, $\beta_4 = 1.18$ and $\beta_5 = 1.22$. This immediately indicates that the triangular lattice has lower free energy than the square lattice which has lower free energy than the 5-fold vortex quasi-crystal (Penrose tiling), as we expected. However, the fact that the free energy difference between the triangular and 5-fold vortex quasi-crystal is only a few percent suggests that appropriate boundaries can favor 5-fold symmetry as the sample size gets smaller, as can appropriately imposed quasi-periodic potentials.

In order to investigate how boundary effects can modify the total free energy of the system, a sample in the shape of a pentagon cylinder of side ℓ and height L is considered. Imposing that no currents flow through the sample boundaries leads to the condition $\hat{\mathbf{n}} \cdot [-i\nabla - 2\pi\mathbf{A}/\Phi_0] \Psi(x, y) = 0$ at all five side faces. The unit vector $\hat{\mathbf{n}}$ points along the normal direction of each facet of the pentagon cylinder. The boundary conditions can be translated in terms of the harmonic function $\gamma(x, y)$ as

$$n_x \frac{\partial \gamma}{\partial y} - n_y \frac{\partial \gamma}{\partial x} = \kappa(n_x y - n_y x), \quad (7)$$

where n_x and n_y are the x and y components of the normal unit vector $\hat{\mathbf{n}}$ at each one of the pentagon cylinder side faces. The solution for this boundary value problem can be obtained using a Schwarz-Christoffel conformal

map of the pentagon into a semi-infinite plane

$$\frac{dz}{dw} = C(w - x_1)^{-2/5}(w^2 - x_2^2)^{-2/5}(w^2 - x_3^2)^{-2/5}, \quad (8)$$

where the vertices of the pentagon located at z_i are mapped into the points $(x_1, \pm x_2, \pm x_3)$ on the real axis of the w -plane. The full solution of this problem is complicated, and requires heavy use of numerical methods [12]. However, the free energy density can be estimated when the bulk solution in Eq. (6) is treated as a variational solution of the boundary value problem determined by Eqs. (3), (7) and (8). The Gibbs free energy density difference $\Delta G = G_3 - G_5$ between the triangular and the 5-fold quasi-periodic Penrose structure then becomes

$$\Delta G = -\frac{1}{8\pi} \frac{(H_{c2} - H)^2}{(2\kappa^2 - 1)\beta^*} + \frac{H_c^2}{4\pi} \epsilon(H), \quad (9)$$

where $\beta^* = \beta_3\beta_5/(\beta_5 - \beta_3)$, H_c is the thermodynamic critical field, and $\epsilon = (\alpha_3 - \alpha_5)(2R_e + \alpha_3 + \alpha_5)/2R_e^2$, with $\alpha_3 = 0.93a_0$, $\alpha_5 = 0.90a_0$, and $a_0 = \sqrt{\Phi_0/H}$. The effective length of the sample $R_e = \ell/\sqrt{4 - \tau^2}$, where $\tau = 2\cos(\pi/5)$ is the golden mean. This expression for ΔG is valid only when $H \gg \Phi_0/R_e^2$. The second term in ΔG takes into account the boundary mismatch energy, and indicates that as the size of the pentagon cylinder gets smaller it becomes more favorable to have a 5-fold quasi-crystal rather than a regular triangular lattice. Notice, however, that when $R_e \rightarrow \infty$ the triangular lattice has lower Gibbs free energy as it must, and no transition to a 5-fold quasi-crystal occurs. Thus, this possible transition may occur for finite sized samples only. From the condition that $\Delta G = 0$ we obtain

$$H_Q = H_{c2} \left[1 - \kappa^* \sqrt{\beta^* \epsilon(H_Q)} \right], \quad (10)$$

where the transition to a quasi-crystal occurs. Here, $\kappa^* = \sqrt{2\kappa^2 - 1}/\kappa$. The phase diagram for a superconductor with $\kappa = 20$, $H_{c2}(0) = 10\text{T}$ and $R_e = 10^{-6}\text{m}$ is shown [13] in Fig. 1 using $H_{c2}(T) = H_{c2}(0) [1 - (T/T_c)^2]$.

The jump of the magnetization $\Delta M (= M_3 - M_5)$ as a function of temperature at the critical field H_Q can be calculated from the Gibbs free energy leading to

$$\Delta M = \frac{H_{c2}}{4\pi} \left[-\frac{\gamma^*}{(2\kappa^2 - 1)\beta^*} + \Delta M_s \right], \quad (11)$$

where $\gamma^* = \kappa^* \sqrt{\beta^* \epsilon}$ and $\Delta M_s = (\alpha_3 - \alpha_5)(R_e + \alpha_3 + \alpha_5)/4\kappa^2 R_e^2 (1 - \gamma^*)$. A plot of ΔM is illustrated in Fig. 2 for the same parameters of Fig. 1. Using these parameters produces jump discontinuities $\Delta M \approx -0.060\text{G}$ at $T = 0$, and $\Delta M \approx -0.028\text{G}$ at $T = 0.8T_c$. (Measurements of ΔM may require the preparation of an array of identical pentagonal cylinders to enhance the value.) Notice that $\Delta M < 0$ indicates that the 5-fold vortex

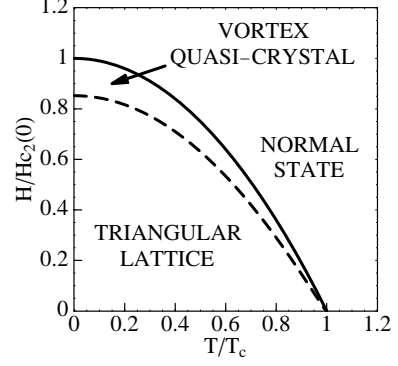


FIG. 1: $H - T$ phase diagram for a pentagonal cylinder cut out of a regular cylinder of radius for $R_e = 10^{-6}\text{m}$. The solid and dashed lines represent H_{c2} and H_Q , respectively, and the superconductor is assumed to have $\kappa = 20$, $H_{c2}(0) = 10\text{T}$.

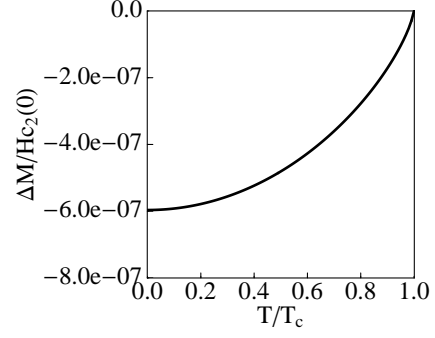


FIG. 2: The jump discontinuity $\Delta M = M_3 - M_5$ at the critical field H_Q for various reduced temperatures T/T_c , using the same parameters of Fig. 1.

quasi-crystal is denser than the triangular vortex lattice at H_Q , being at best a few percent denser at $T = 0$.

In addition to magnetization measurements, it is also interesting to perform calorimetric experiments. However, specific heat measurements are very difficult because they require large samples. Since sample size is important for the present discussion it is not clear that such experiments can be successfully performed. Nevertheless, the thermodynamic relationship between the magnetization and entropy jumps is revealed in the Clapeyron equation $\Delta S = S_3 - S_5 = -\Delta M dH_Q/dT$. Since $dH_Q/dT < 0$, and $\Delta M < 0$ implies that $\Delta S < 0$, the entropy S_3 of the triangular vortex lattice is less than the entropy S_5 of the 5-fold vortex quasi-crystal, indicating that latent heat $L = T\Delta S$ is required to cause this phase transition.

Thermodynamic quantities can provide a good understanding of properties averaged over the entire sample. However, the use of local probes is much desired in order to reveal the change in structure from a triangular vortex crystal to a 5-fold vortex quasi-crystal. Thus, neu-

neutron scattering, Bitter decoration and scanning tunneling microscopy (STM) experiments can help elucidate the structure of the vortex arrangement.

In neutron diffraction experiments periodic or quasi-periodic variations of $\mathcal{H}(x, y)$ will result in Bragg peaks. The position of these peaks determine the characteristic length scale of the vortex structure and its symmetry. The neutron scattering amplitude in the Born approximation is

$$b(\mathbf{q}) = \frac{M_n}{2\pi\hbar^2} \int \mu_n H(\mathbf{r}) \exp(i\mathbf{q} \cdot \mathbf{r}) d\mathbf{r}, \quad (12)$$

where $\mu_n = 1.91e\hbar/M_n c$ is the neutron magnetic moment and the M_n is the neutron mass. The scattering amplitude $b(\mathbf{q})$ is directly proportional to the Fourier transform $H(\mathbf{q})$ [$\mathcal{H}(q_x, q_y)$] of the microscopic field $H(\mathbf{r})$ [$\mathcal{H}(x, y)$] of Eq. (2). The neutron scattering cross section $\sigma(q_x, q_y) = 4\pi^2 |b(q_x, q_y)|^2$ has sharp peaks at $(q_x, q_y) = (0, 0)$ (central peak) and at $(q_x, q_y) = (\pm q_{xNm}, \pm q_{yNm})$ (first Bragg peaks), where $q_{xNm} = Q_N \cos(m\pi/N)$ and $q_{yNm} = Q_N \sin(m\pi/N)$, with $m = 0, 1, \dots, N-1$. For the triangular lattice $N = 3$ the first Bragg peak occurs at $|Q_3| = 2.31 \times \pi/d_3$, where d_3 is the lattice spacing. For the 5-fold vortex quasi-crystal (Penrose Lattice, $N = 5$) the first Bragg peak occurs at $|Q_5| = 2.46 \times \pi/d_5$, where d_5 is the side of a tile. Since the sample size is important for the observation of a 5-fold quasi-crystal, neutron scattering experiments may be difficult to perform. Thus, Bitter decoration or STM may be better techniques. For instance, STM scans at different fields and temperatures in the vicinity of $H_Q(T)$ should reveal the real space locations of vortices, which can be Fourier transformed (FT) to obtain a 6-fold pattern for the triangular vortex lattice and a 10-fold pattern for the 5-fold vortex quasi-crystal (Penrose lattice), see Fig. 3.

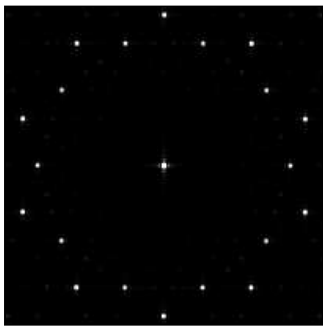


FIG. 3: First peaks of the square of the FT pattern for the 5-fold vortex quasi-crystal (Penrose lattice). Notice the 10-fold symmetry revealed.

Now that the phase diagram, thermodynamics, and the local signatures of a vortex quasi-crystal have been discussed, it is important to say a word on the stability of such structures. A stability analysis in the free energy can be performed by moving the vortices away from

their equilibrium positions z_i to $z_i + \delta z_i$. The eigenvalues associated with these displacements indicates that for $H > H_Q(T)$ the vortex quasi-crystal lattice is stable. However, there is no full compatibility of the 5-fold vortex lattice with the pentagon cylinder geometry, and thus the appearance of disclinations and dislocations is possible. As a result there is an additional possibility of the coexistence of a solid (crystal or quasi-crystal) vortex phase in the center of the sample and a liquid vortex phase closer to the edges.

In conclusion, we have shown that vortex quasi-crystals may be experimentally observed in isotropic type II superconductors, provided that the sample size and shape are properly chosen. This result opens the possibility of a new phase of vortex matter: the vortex quasi-crystal. This yet non-observed phase adds to the many phases of vortex matter already seen experimentally, the vortex crystal, the vortex liquid [14, 15] and the vortex glass [16]. By taking into account boundary effects, sample shape and size or properly imposed quasi-periodic potentials, the present work suggests that a vortex quasi-crystal phase may exist and compete with vortex liquid, glass or crystal phases, as magnetic field, temperature and disorder are varied.

We would like to thank Wai Kwok for references, the Aspen Center for Physics for their hospitality, and NSF (DMR-0304380) for financial support.

-
- [1] G. W. Crabtree and D. R. Nelson, *Physics Today*, pp. 38-45, April (1997).
 - [2] D. Schechtman, I. Blech, D. Gratias, and J. W. Cahn, *Phys. Rev. Lett.* **53**, 1951 (1984).
 - [3] M. R. Matthews *et al.*, *Phys. Rev. Lett.* **83**, 2498 (1999).
 - [4] M. W. Zwierlein, J. R. Abo-Shaeer, A. Schirotzek, C. H. Schunck, and W. Ketterle, *Nature* **435**, 1047 (2005).
 - [5] A. K. Geim *et al.*, *Nature* **390**, 259 (1997).
 - [6] A. K. Geim *et al.*, *Phys. Rev. Lett.* **85**, 1528 (2000).
 - [7] L. F. Chibotaru, A. Ceulemans, V. Bruyndoncx, and V. V. Moshchalkov, *Nature* **408**, 833 (2001); *Phys. Rev. Lett.* **86**, 1323 (2001).
 - [8] D. A. Dikin, V. Chandrasekhar, V. R. Misko, V. M. Fomin, and J. T. Devreese, *Eur. Phys. J. B* **34**, 231 (2003).
 - [9] The term “first order phase transition” appear in quotes since the sample size is finite.
 - [10] D. Saint-James, G. Sarma, and E. J. Thomas, *Type II superconductivity*, chap. 3, pp. 52-62, Pergamon Press, Oxford (1969).
 - [11] A. A. Abrikosov, *Sov. Phys. JETP* **5**, 1174 (1957).
 - [12] P. Henrici, *Applied and computational complex analysis*, vol III, chap. 16, John Wiley and Sons, New York (1986).
 - [13] The critical field $H_{c3}(T)$ for surface superconductivity is not shown in Fig. 1.
 - [14] H. Safar *et al.*, *Phys. Rev. Lett.* **70**, 3800 (1993).
 - [15] W. K. Kwok *et al.*, *Phys. Rev. Lett.* **72**, 1092 (1994).
 - [16] R. H. Koch *et al.*, *Phys. Rev. Lett.* **63**, 1511 (1989).